ground water

Modeling Axisymmetric Flow and Transport

by Christian D. Langevin

Abstract

Unmodified versions of common computer programs such as MODFLOW, MT3DMS, and SEAWAT that use Cartesian geometry can accurately simulate axially symmetric ground water flow and solute transport. Axisymmetric flow and transport are simulated by adjusting several input parameters to account for the increase in flow area with radial distance from the injection or extraction well. Logarithmic weighting of interblock transmissivity, a standard option in MODFLOW, can be used for axisymmetric models to represent the linear change in hydraulic conductance within a single finite-difference cell. Results from three test problems (ground water extraction, an aquifer push-pull test, and upconing of saline water into an extraction well) show good agreement with analytical solutions or with results from other numerical models designed specifically to simulate the axisymmetric geometry. Axisymmetric models are not commonly used but can offer an efficient alternative to full three-dimensional models, provided the assumption of axial symmetry can be justified. For the upconing problem, the axisymmetric model was more than 1000 times faster than an equivalent three-dimensional model. Computational gains with the axisymmetric models may be useful for quickly determining appropriate levels of grid resolution for three-dimensional models and for estimating aquifer parameters from field tests.

Introduction

Under homogeneous conditions and in the absence of a regional hydraulic gradient, ground water flow to an extraction well or away from an injection well exhibits radial symmetry. This radial symmetry has provided the foundation for characterizing aquifer properties from aquifer tests. Radial symmetry reduces the governing flow equation by one dimension. For numerical simulations, which can be encumbered by lengthy computer runtimes, reducing the number of dimensions can substantially reduce computer runtimes. These types of simulations are called cylindrical, radial, or axisymmetric simulations. For aquifers with strong regional flow fields, spatially distributed aquifer stresses, or lateral variations in hydraulic properties, the assumption of axial symmetry cannot be justified. In many cases, however, the assumption of axial symmetry is based on parsimony, and in the absence of conflicting evidence, it can be reasonably assumed as a first approximation. This paper focuses on those conditions where axial symmetry can be reasonably assumed.

Axisymmetric flow and transport simulations run much faster than their full three-dimensional counterparts, but surprisingly, they are not commonly used. Most reported applications have been with parameter estimation techniques to estimate hydraulic properties from aquifer tests (Lebbe et al. 1992; Lebbe and De Breuck 1995, 1997; Lebbe 1999; Lebbe and van Meir 2000; van Meir and Lebbe 2005; Halford and Yobbi 2006). The axisymmetric approach is attractive for this type of application because the forward model must run quickly. An obvious reason for their lack of widespread use is that they are limited by the assumption of radial symmetry. Another explanation for their lack of use is that there is a perception that specialized computer programs are required to simulate axisymmetric flow. The purpose of this paper is to show that common modeling programs can be used to perform accurate simulations of ground water flow, flow and transport, and coupled variable-density flow and transport.

Simulation of axisymmetric flow with the finite-element method is relatively straightforward. Finite-element meshes can easily be developed to represent the radially convergent or radially divergent flow and transport patterns that result from extraction or injection wells. Finite-element programs perform integration over each

Florida Integrated Science Center, U.S. Geological Survey, 3110 SW 9th Avenue, Fort Lauderdale, FL 33312; (954) 377-5900; fax: (954) 377-5901; langevin@usgs.gov

Received October 2007, accepted February 2008.

doi: 10.1111/j.1745-6584.2008.00445.x

element, and thus, as long as the element is properly shaped, there are no special considerations for simulating axisymmetric flow. The SUTRA code (Voss 1984; Voss and Provost 2002), for example, naturally represents axisymmetric flow when the mesh is designed to represent the gradual increase in flow area in the radial direction. Other finite-element codes, such as RADFLOW (Reilly 1984), FEFLOW (Diersch 2002), and FEAS (Zhou 1999; Bensabat et al. 2000), among others, are also capable of simulating axisymmetric flow.

The finite-difference method can also be used to solve a radial form of the governing flow equation (Cooley 1971; Rushton and Redshaw 1979). For example, van Meir (2001) added solute transport capabilities to an axisymmetric finite-difference program (Lebbe 1999). The original MODFLOW program (McDonald and Harbaugh 1988) and subsequent versions (Harbaugh and McDonald 1996; Harbaugh et al. 2000; Harbaugh 2005), however, are based on a rectangular finite-difference grid. Therefore, this commonly used program cannot be directly used to simulate axisymmetric flow. For this reason, investigators have developed simple methods for tricking MODFLOW into simulating axisymmetric flow (Anderson and Woessner 1992). Transmissive and storage properties are increased with radial distance from the pumping well to simulate the increasing flow area and storage volume (Land 1977). Anderson and Woessner (1992) briefly describe the procedure for developing an axisymmetric flow model with this approach.

A subtle problem with tricking standard versions of MODFLOW to simulate axisymmetric flow was addressed by Reilly and Harbaugh (1993). MODFLOW calculates the hydraulic conductance between cells by averaging transmissivity values. For axisymmetric flow, the hydraulic conductance varies linearly between two adjacent nodes; therefore, the use of harmonic averaging (derived for piecewise variation in transmissivity) underestimates the conductance between two nodes. Logarithmic averaging has been shown to provide the correct head distribution for a linear variation in transmissivity (Appel 1976; Goode and Appel 1992). Reilly and Harbaugh (1993) developed the RADMOD preprocessor for MODFLOW, which calculates interblock conductance using the logarithmic mean and writes the conductance values in a special Generalized Finite-Difference (GFD) package that is then read by MODFLOW. Because conductances are preprocessed and, therefore, are not calculated as a function of saturated thickness during the simulation, the RADMOD approach is limited to confined conditions and unconfined conditions where drawdowns are relatively small compared to the saturated layer thickness. The RADMOD approach is not commonly used, and the GFD package is no longer included in MODFLOW (e.g., MODFLOW-2000 or MODFLOW-2005). As shown here, the logarithmic interblock transmissivity weighting option, which is included with the Block-Centered Flow (BCF) and Layer Property Flow (LPF) packages of MODFLOW-2000 and MODFLOW-2005, can be used to calculate accurate hydraulic conductances for axisymmetric models.

Recently, Samani et al. (2004) embedded a log-scaling method (LSM) into MODFLOW-2000 to simulate axisymmetric flow. The LSM is based on a set of scale factors derived by comparing the governing equations in Cartesian and cylindrical coordinates. Samani et al. (2004) tested the LSM with several different radial flow problems that varied in complexity. For the problems tested, the drawdowns calculated by LSM compared well with drawdowns from analytical solutions and RADMOD. Another MODFLOW development effort that is relevant to axisymmetric simulations is that of Romero and Silver (2006), who tested a curvilinear version of MODFLOW-88 with a radial flow problem. Their implementation was developed in a robust manner so that a MODFLOW finite-difference grid can conform to curved boundaries. Presumably, a single row could be used with this program to represent a wedge, provided that the code was modified to calculate intercell conductances using the RADMOD approach.

This paper shows that unmodified versions of common computer programs, such as MODFLOW, MT3DMS, and SEAWAT, accurately simulate axisymmetric ground water flow, flow and transport, and coupled variable-density flow and transport. By adjusting several input parameters to account for the cylindrical geometry and by selecting the appropriate weighting scheme, MODFLOW (Harbaugh et al. 2000; Harbaugh 2005) is shown to be fully capable of representing axisymmetric flow. In addition to ground water flow, MT3DMS (Zheng and Wang 1999) can also be used with this approach to represent axially symmetric solute transport. This approach can be extended to represent axisymmetric variable-density flow and transport with the MODFLOW/MT3DMS-based SEAWAT computer program (Guo and Langevin 2002; Langevin et al. 2003; Langevin and Guo 2006). The simple method is demonstrated for three different classes of problems: (1) flow; (2) flow and transport; and (3) coupled flow and transport. For each example problem, results are compared with analytical solutions and other numerical solutions.

Methods

Axisymmetric modeling with MODFLOW, MT3DMS, and SEAWAT is conceptually straightforward. It involves a simple modification of several input parameters to account for the discrepancy between the intended cylindrical geometry and the rectangular geometry upon which these programs are based. Modification of the source code is not required, although a simple package could be developed to simplify data input. The presence of lateral heterogeneities in aquifer properties cannot be represented with this approach, but it is possible to represent a system with layered heterogeneity.

An axisymmetric model can be developed to represent one-dimensional radial flow or two-dimensional flow in a vertical cross section. For one-dimensional flow, a single layer would be used with multiple columns or multiple rows. For two-dimensional flow in a vertical cross section, a single layer has been used with multiple columns and rows. The layer is conceptualized as being flipped upright to represent a cross section (Anderson and Woessner 1992). This was the approach used by Halford and Yobbi (2006) and Halford et al. (2006) and has some advantages in the preparation of input data sets. In this paper, two-dimensional flow in a vertical cross section is represented using multiple layers, one row, and multiple columns (multiple rows and single column could also be used). There are several reasons for selecting this profile orientation as opposed to flipping a single layer upright: (1) model layers can be confined, unconfined, or convertible; (2) cells can dry and rewet; (3) the logarithmic weighting scheme used to calculate interblock transmissivity is used only in the radial direction and not the vertical direction (the rationale for using the logarithmic weighting scheme is discussed later); and (4) some programs, such as SEAWAT, require correct layer top and bottom elevations.

The finite-difference grid for an axially symmetric profile model is shown in Figure 1. The r-axis is horizontal with increasing values away from the well. The vertical z-axis is positive in the upward direction. The indices j and k represent model columns and layers, respectively. The equations presented here assume that the well is located in one or more layers of column 1. Because of the assumed axially symmetric conditions, the profile model can be thought of as representing a slice (or wedge) or as a full cylinder. The value selected for the angle, θ, is arbitrary and does not affect the solution. For the example problems shown later, θ is set to 2π, and thus each cell can be thought of as a ring with a width equal to the cell width (Figure 1).

For a standard profile model with a single row, MODFLOW calculates the area of cell j as $A_j^p = \mathrm{DELR}_j \cdot \mathrm{DELC}$, where DELR_j is the width of column j and DELC is the width of the row. DELC is normally set to a value of 1 for standard cross section models and should be set to a value of 1 for axisymmetric profile models when using the equations presented here. For an axisymmetric profile model, the area of cell j is $A_j^a = \mathrm{DELR}_j \theta r_j$. With the approach here, adjustments to account for the variation of A_j^a are made to all input values used in equations that contain an area or volume.

Parameter Adjustment for Horizontal Flow

MODFLOW uses the following formulation for hydraulic conductance along a row (CR):

$$\mathrm{CR}_j = \frac{2 \cdot \mathrm{DELC} \cdot T_{j+1/2}}{\mathrm{DELR}_j + \mathrm{DELR}_{j+1}} \tag{1}$$

Depending on the assumed spatial distribution for hydraulic conductivity (Goode and Appel 1992), interblock transmissivity (T) can be calculated in MODFLOW using several different weighting options. When using the LPF package, the LAYAVG flag corresponds to the following weighting options: (1) harmonic mean; (2) logarithmic mean; or (3) arithmetic mean of saturated thickness and logarithmic mean hydraulic conductivity.

The BCF package also has these weighting options, although the flag name and numeric values are different. For confined conditions and a LAYAVG value of 2 (or 3 since the saturated thickness equals the aquifer thickness for confined conditions), the interblock transmissivity is calculated as follows:

$$T_{j+1/2} = \frac{T_{j+1} - T_j}{\ln\left(\dfrac{T_{j+1}}{T_j}\right)} \tag{2}$$

For confined conditions, transmissivity is the product of horizontal hydraulic conductivity and layer thickness. Thus, the transmissivity value calculated by MODFLOW for cell j is as follows:

$$T_j = K_{h,j}^{*} \Delta z \tag{3}$$

where $K_{h,j}^{*}$ is the horizontal hydraulic conductivity value entered as input to MODFLOW.

For MODFLOW to simulate axisymmetric flow, the horizontal hydraulic conductivity value of the aquifer (K_h) is entered as input to the model as a function of radial distance:

$$K_{h,j}^{*} = r_j \theta K_{\mathrm{h}}, \tag{4}$$

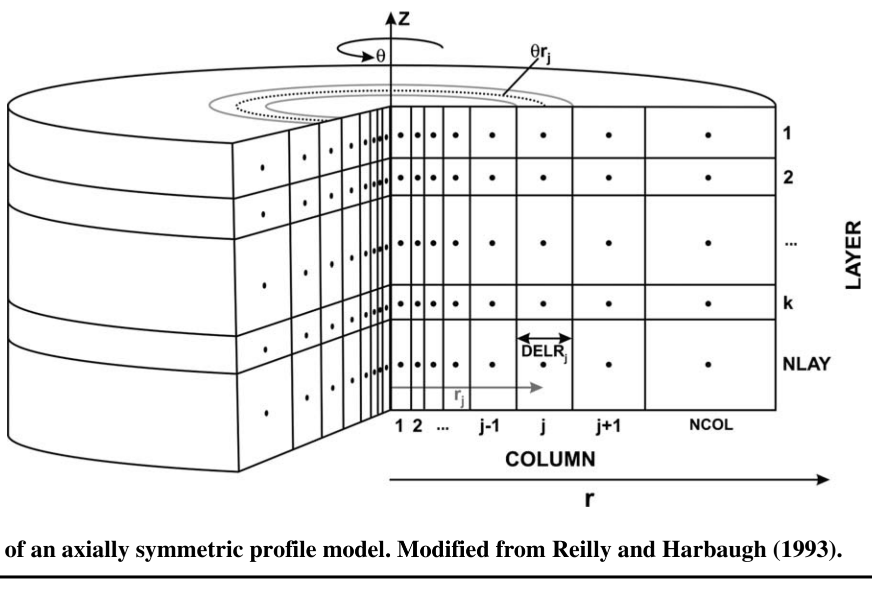

Figure 1. Schematic of an axially symmetric profile model. Modified from Reilly and Harbaugh (1993).

where r_j is the radial distance between the model edge and the center of cell j, and θ is the angle open to flow, which is typically 2π. By calculating the transmissivity values in Equation 2 using Equations 3 and 4, substituting the resulting expression into Equation 1, and noting that:

$$\frac{1}{2}(\mathrm{DELR}_j + \mathrm{DELR}_{j+1}) = r_{j+1} - r_j \qquad (5)$$

then the expression for conductance along a row is as follows:

$$\mathrm{CR}_j = \frac{\theta K_h \Delta z}{\ln\left(\frac{r_{j+1}}{r_j}\right)} \qquad (6)$$

If θ is set to 2π, then Equation 6 is identical to the conductance equation presented by Reilly and Harbaugh (1993) and can be derived from the Thiem equation or from the limit of many radial conductance terms in series (Bennett et al. 1990).

The default harmonic weighting option in MODFLOW is not equivalent to Equation 6 because linear change in conductance within a single finite-difference cell is not simulated. Predicted drawdown, particularly near the well, will be overestimated by harmonic averaging. Logarithmic averaging better approximates analytical solutions and should be the preferred method for simulating axisymmetric flow and transport.

Axially symmetric flow for unconfined conditions (which cannot be represented with RADMOD if drawdowns are large) can also be accurately simulated using the standard version of MODFLOW by setting LAYAVG equal to 3. With this weighting option, the saturated thickness at the $j+1/2$ location in the grid is calculated using the arithmetic average of the saturated thickness at cell j and $j+1$. The effect of the linear increase in flow area as a function of radial distance from the well, however, is taken into account by using the logarithmic average. Although it is possible to represent axisymmetric flow for unconfined conditions, it is often preferable to approximate the system as confined, particularly during parameter estimation. This is justified if the drawdown is small relative to the saturated thickness of the model layer.

Parameter Adjustment for Vertical Flow, Storage, and Advective Flow Velocity

Similar adjustments also are required for vertical hydraulic conductivity, specific storage, and, in the case of transport, porosity (n). For example, specific storage must be entered into MODFLOW as follows:

$$Ss_j^* = Ss_j \frac{A_j^a}{\mathrm{DELR}_j} = Ss_j \theta r_j \qquad (7)$$

Specific yield follows a similar adjustment. Likewise, vertical hydraulic conductivity is entered as follows:

$$K_{v,j}^* = K_{v,j} \theta r_j \qquad (8)$$

Within MODFLOW, changes in storage and vertical conductance are calculated by multiplying specific storage and vertical hydraulic conductivity, respectively, by the cell area (Harbaugh et al. 2000, equations 34 and 25).

To represent transport using MT3DMS as a standalone program or within SEAWAT, porosity must also be adjusted. The adjustment follows the same procedure as for the other input parameters:

$$n_j^* = n_j \theta r_j \qquad (9)$$

The scope of this paper is limited to advective and dispersive transport, but presumably several other input parameters could follow a similar adjustment in order to represent optional processes included in the MT3DMS Reactions Package (adsorption, decay, and dual-domain transport).

Specification of Sources and Sinks

Sources and sinks also must be specified carefully so that the fluxes conform to the intended axisymmetric geometry. To specify a well injection or extraction, the discharge value is adjusted to account for the relative proportion of the slice by multiplying the value by $\theta/2\pi$. For the problems tested here, θ is assigned a value of 2π, and thus the actual well discharges are used as input to the model. Injection and extraction wells may be fully or partially penetrating. The most common way of apportioning the total well flux among the model layers is to weight by transmissivity. Another option is to assign a relatively large vertical hydraulic conductivity value to the cells that represent the borehole and then apply the flux to a single well cell (Halford et al. 2006; Langevin and Zygnerski 2006). Flow within the borehole is then distributed by the model.

Model input values for aerially distributed sources or sinks such as recharge and evapotranspiration require minor adjustments to account for the cell area. Accordingly, recharge, evapotranspiration, and any other aerially distributed fluxes are multiplied by $r_j\,\theta$.

Considerations for Spatial Resolution

Accurate representation of the large hydraulic gradients that occur near an injection or extraction well can require a fine horizontal and vertical discretization. This is often one reason for considering the use of an axisymmetric model since development of a full three-dimensional representation can be computationally demanding due to the large number of grid cells. A common approach for designing the finite-difference grid for an axisymmetric representation is to set the first column width equal to the well radius and then use an expansion factor (α) to increase cell widths away from the well. This was the approach implemented in RADMOD, in which a constant α value, obtained through experimentation, is used to design the grid. Barrash and Dougherty (1997) suggested a slight variation in that while the first cell width should be set equal to the well radius, the width of the second cell may need to be set to a value less than the well radius. The widths of the remaining cells can then be calculated using an expansion factor. For simulations that include transport, a constant expansion factor may not be appropriate, and a high level of discretization may be required for any cells that undergo changes in concentration due to injection or extraction. For these types of simulations, Courant and Peclet criteria can offer some insight into appropriate levels of resolution (Zheng and Bennett 2002), but there is no clear way to determine, a priori, the level of resolution that yields the best compromise between accuracy and computer runtimes. Appropriate levels of resolution for transport studies are often determined through a grid convergence analysis. The approach presented here will work with a variety of different discretization schemes.

Test Problems

Test problems from the literature were selected to assess the accuracy of the radial approach for three different types of problems: (1) ground water flow; (2) ground water flow and solute transport; and (3) coupled variable-density ground water flow and solute transport. Specifically, the following problems were tested:

- Ground water extraction—constant-density ground water flow to an extraction well (Samani et al. 2004).
  - Case 1—steady flow to a fully penetrating well.
  - Case 2—unsteady flow to a partially penetrating well.
- Push-pull test—constant-density ground water flow and solute transport (Schroth and Istok 2005).
- Upconing of dense saline ground water—variable-density ground water flow and solute transport to a partially penetrating well (Zhou et al. 2005).

The unmodified version of MODFLOW-2000 was used for the ground water extraction simulations. Unmodified versions of MODFLOW-2000 and MT3DMS were used for the push-pull test simulations. The unmodified version of SEAWAT was used for the upconing simulations.

Ground Water Extraction

Two cases of ground water extraction are presented here to demonstrate the accuracy of using the standard version of MODFLOW to simulate axisymmetric ground water flow. These two cases are patterned after the problems described by Samani et al. (2004).

Case 1—Steady Flow to a Fully Penetrating Well

For case 1, steady flow to a fully penetrating well is considered for both confined and unconfined conditions. In both cases, flow is treated as one dimensional. Input parameters for the confined simulation are based on the first example problem considered by Samani et al. (2004). The extraction rate is 6.28×10^{-4} m^3/s, and the aquifer is homogeneous and isotropic with a hydraulic conductivity value of 1×10^{-4} m/s. For the confined simulation, the aquifer is 8 m thick.

The problem was tested with several different grid configurations, which consisted of various levels of resolution and grid expansion factors; however, for this analysis, a single-layer model with one row and 15 columns provides a reasonable solution to the problem. The cell in the first column has a width of 0.1 m. Subsequent cell widths increase by a factor of 1.302, which places the center of the 15th column at a radial distance of 15 m. A constant head boundary with a value of 10 m was assigned to column 15.

Results from the confined and unconfined simulations are compared with the results from the Thiem analytical solution in Figures 2 and 3, respectively. An important consideration here is that the Thiem solution provides a drawdown estimate for any radial distance given the drawdown at a specified distance (drawdown is specified as zero at $r = 15$ m). For both cases, results from the MODFLOW simulations compare better with the analytical solution when the logarithmic averaging

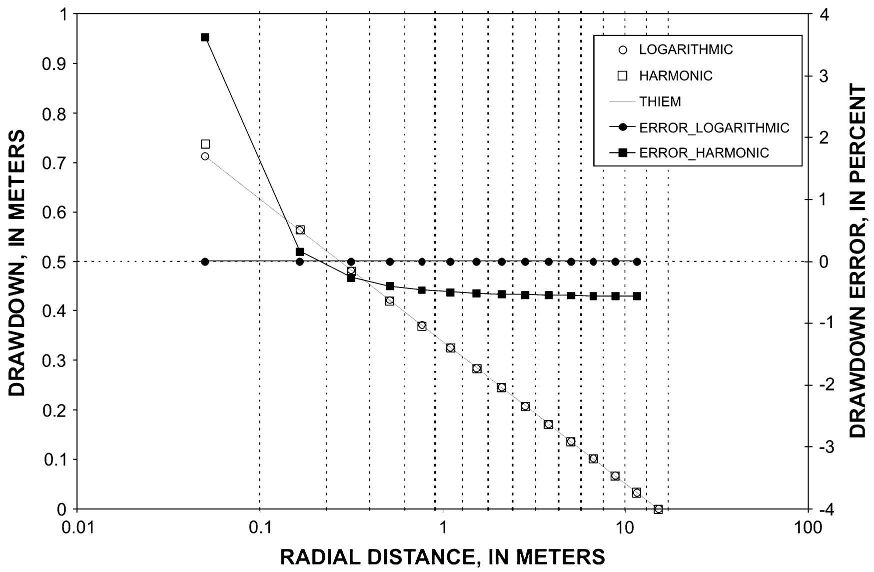

Figure 2. Plot of drawdown vs. distance for one-dimensional flow in a confined aquifer. The numerical solution is shown for simulations using harmonic averaging and logarithmic averaging. The Thiem analytical solution is also shown and was used to calculate the error in the numerical solutions. The finite-difference grid is shown with vertical dashed lines.

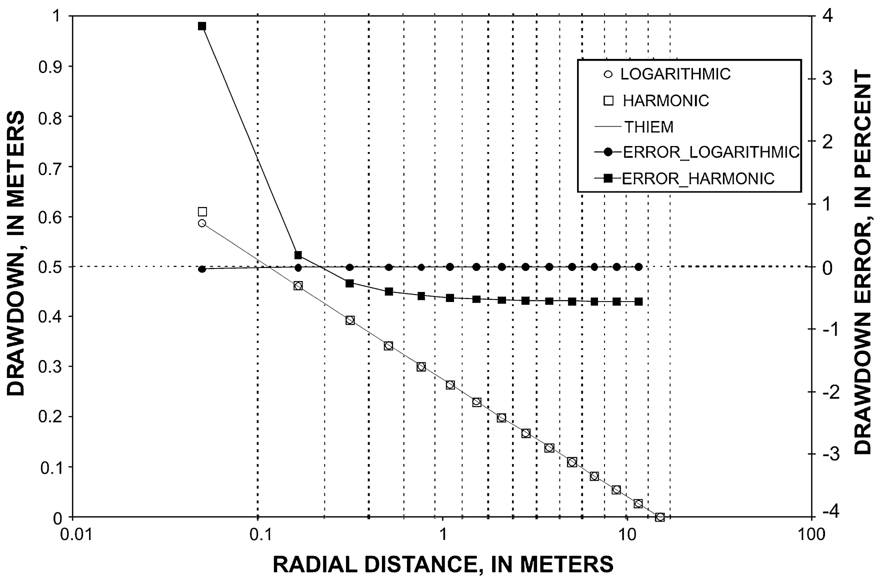

Figure 3. Drawdown vs. distance for one-dimensional flow in an unconfined aquifer. The numerical solution is shown for simulations using harmonic averaging and logarithmic averaging. The Thiem analytical solution is also shown and was used to calculate the error in the numerical solutions. The finite-difference grid is shown with vertical dashed lines.

option is used. When the harmonic averaging option is used, the error (relative to the analytical solution) in calculated drawdown is nearly 4%. These drawdown errors are positive near the well (indicating an overestimate in drawdown) and become negative within a few model cells of the extraction well. Drawdown errors for the simulations with logarithmic averaging are less than one hundredth of a percent over the entire distance.

Case 2—Unsteady Unconfined Flow to a Partially Penetrating Well

Extraction from a partially penetrating well in an 8-m-thick unconfined aquifer was simulated for case 2. Unsteady flow in the radial and vertical directions was simulated as initially presented in Samani et al. (2004). The extraction well is open from 0.8 to 3.2 m above the aquifer base and extracts at a rate of 6.28×10^{-5} m^3/s (Figure 4). The aquifer is isotropic and homogeneous

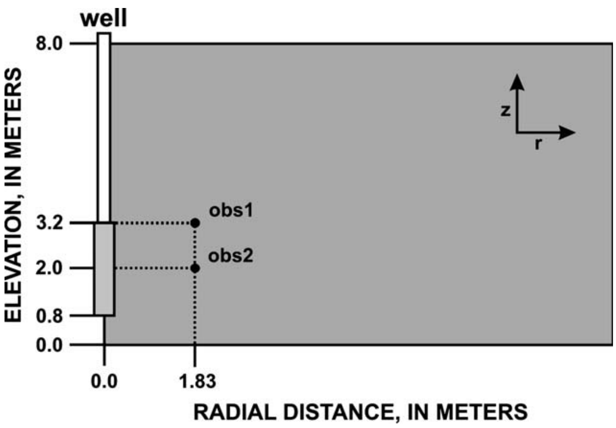

Figure 4. Schematic for case 2 of the ground water extraction problem. Open-hole interval of the well is shown in light gray.

with a hydraulic conductivity, specific storage, and specified yield of 1×10^{-5} m/s, 1.03155×10^{-3}/m, and 0.2, respectively. Drawdown is evaluated at two observations points located 1.83 m from the pumping well. Observation 1 (obs1) is at an elevation of 3.2 m. Observation 2 (obs2) is at an elevation of 2.0 m.

Samani et al. (2004) simulated the problem using two different representations of the spatial and temporal resolution. A "short" simulation with a refined grid near the extraction well was used to evaluate early-time flow characteristics near the well. A "long" simulation with a longer (but less refined) grid and with more time steps was used to characterize the longer term response of the aquifer. Where possible, the temporal and spatial discretization parameters used here were selected to match those used by Samani et al. (2004). For both the short and the long simulations, the grid consisted of 43 columns and 77 layers. Both simulations used the same vertical resolution, which had layer thicknesses of 0.001 m resolution at the top and bottom of the well screen. Upward from the well screen, layer thicknesses increased using a multiplier of 1.387. Downward from the well screen, layer thicknesses increased using a multiplier of 1.41. Layer thicknesses also increased from the bottom of the well screen toward the center of the well using a multiplier of 1.40. Water was extracted proportionally to layer thickness between layers 24 and 60. The column width for the first column ($DELR_1$) was specified as 0.001 m. For the short simulation, the column widths expanded using a multiplier of 1.430. For the long simulation, the column widths expanded using a multiplier of 1.482. For both simulations, a constant head value of 8.0 m was assigned to the last column. For the short simulation, a period length of 19,943 s was divided into 295 time steps using a time step multiplier of 1.03663. For the long simulation, a period length of 6.602×10^7 s was divided into 36 time steps using a time step multiplier of 1.58489.

To evaluate the accuracy of the numerical solution for this problem, the WTAQ computer program (Barlow and Moench 1999) was used to calculate drawdowns as a function of radial distance from the well for a specific time and as a function of time for a specific location. An accuracy ratio (AR), which is a measure of the relative error, was calculated using the equation in Samani et al. (2004):

$$\mathrm{AR} = \left(\frac{|h_\mathrm{L} - h_\mathrm{A}|}{J}\right) \times 100 \qquad (10)$$

where h_L is the numerically calculated head, h_A is the head calculated using an analytical solution, and J is some reference value based on length characteristic of the problem.

Drawdowns that were simulated with MODFLOW at obs1 and obs2 after 19,943 s of pumping differed from analytical results by less than 0.2% (Figure 5). The worst AR (calculated using a representative drawdown value of $J = 2.5$ m) is 0.23%. Samani et al (2004) reported problems with the total mass balance in that the error could not be reduced below 8.52%. For the simulation reported here, the total mass balance discrepancy was −0.25%. Drawdowns after 19,943 s of pumping were presented, so these results are directly comparable to Samani et al. (2004, figure 9).

Results for the long simulation are shown for obs1 as a drawdown-time plot in Figure 6. This figure can be compared directly with figure 11 in Samani et al. (2004). Good agreement is again obtained between MODFLOW and the analytical solution. The worst AR, calculated using $J = 1.0$ m (approximate drawdown at the end of the simulation), is less than 2%. The worst AR reported by Samani et al. (2004) was similar. For obs2, the worst AR calculated from the MODFLOW results was also less than 2%.

Push-Pull Test

Injection and extraction from a single well, called a push-pull test, can be used for in situ determination of a variety of aquifer properties (Schroth and Istok 2006). Schroth and Istok (2005) presented an analytical solution for a spherical flow push-pull test where water is injected at a point and then recovered. The analytical solution includes the effects of mechanical dispersion in the longitudinal direction (by definition there should be no transverse mixing for this problem) as the solute sphere expands due to injection and then contracts due to extraction. To test their analytical solution, Schroth and Istok (2005) developed a simple example problem and showed that the results from the STOMP numerical model (White and Oostrom 2000) were in good agreement with the results of the analytical solution. The Schroth and Istok (2005) spherical solution is based on the earlier representation of one-dimensional cylindrical flow (Gelhar and Collins 1971). The example problem of Schroth and Istok (2005) is used here to test the radial flow and transport modeling approach presented in this paper.

The example problem consists of injection of a solute into a homogeneous and isotropic aquifer. The computational domain extends from $r = 0$ to $r = 605$ cm using a 5-cm spacing (121 cells in the radial direction). A 5-cm grid resolution is also used in the vertical direction with 121 cells. This grid contains a higher level of resolution and a larger domain in the vertical direction than that used by the Schroth and Istok (2005) in their STOMP simulations. This revised grid is used here to improve accuracy and minimize boundary effects. Injection and extraction at a rate of 23.14 cm^3/s is assigned to a single cell at the left boundary halfway between the top and the bottom of the model. Injection occurs for 1 d; extraction occurs for 2 d. Constant head cells with a prescribed inflow solute concentration of zero were placed along the top, bottom, and right side boundaries. The head assigned

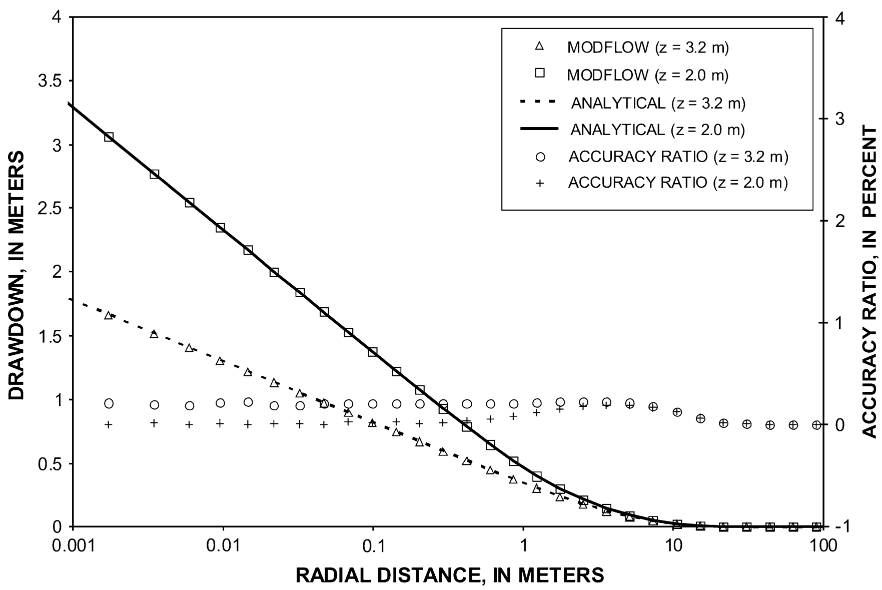

Figure 5. Drawdown-distance plot for the case of unsteady unconfined flow to a partially penetrating well. Plot is for time = 19,943 s.

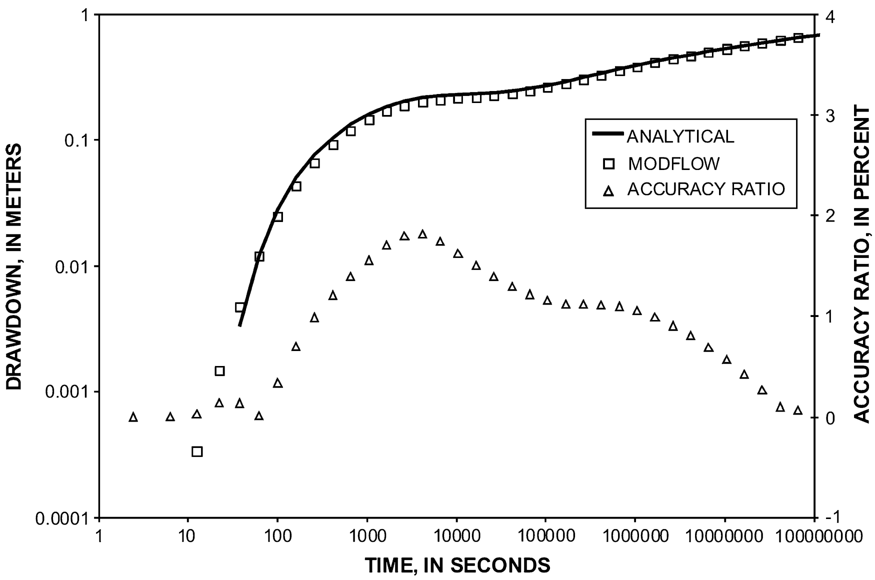

Figure 6. Drawdown-time plot for the case of unsteady unconfined flow to a partially penetrating well. Plot is for obs1.

to these cells was calculated based on the radial distance from the well to the boundary using a three-dimensional form of the Thiem equation. This procedure ensured that spherical flow patterns were calculated by the model and was a substantial improvement over previous simulations with various combinations of no-flow and constant head boundaries. Any hydraulic conductivity value can be used for the problem; a value of 1 cm/s was used for these simulations. A uniform value of 0.4 was used for porosity. Specific storage was set to zero. For these simulations, the finite-difference scheme with upstream weighting was used to solve the solute transport equation using transport time steps calculated from a specified grid courant value of 0.50.

Numerical results were compared first with a simple analytical solution for an expanding and contracting sphere. This comparison is possible because the specific storage is specified as zero. The numerical results were then compared with Schroth and Istok (2005) analytical solution for the concentration breakthrough curve at the well. The analytical equation for the radius of the sphere of injected water was calculated as a function of time using the injected (or withdrawn) volume and the porosity. Sphere radii to the 0.5 normalized concentration value were also calculated by interpolating results of the numerical model. Injected sphere radii were calculated for three lines extending outward from the injection well: the z direction, the r direction, and the r to z direction (a line at 45° to the r direction). When plotted against time, the simulated sphere radii show good agreement with the analytical solution (Figure 7). An exception to this is for later times when the extracted volume approaches the injected volume. This discrepancy appears to be due to numerical dispersion that results when the outer edges of the sphere are drawn into the highly convergent flow field near the extraction point. Increasing the grid resolution near the extraction point would likely improve the numerical results. The simulated concentration breakthrough curve at the well is in good agreement with the Schroth and Istok (2005) analytical solution (Figure 8). There is a slight discrepancy between the numerical and analytical results. A nearly identical discrepancy was shown by Schroth and Istok (2005) in their comparison of the analytical solution with the simulated results from the STOMP program.

Upconing of Dense Saline Ground Water

An upconing problem from the literature was selected to demonstrate the radial approach for a variable-density system. Zhou et al. (2005) applied the FEAS code to a hypothetical upconing problem where a partially penetrating well extracts water from the upper fresh water part of a confined aquifer. Over time, saline water beneath the well is gradually drawn upward. Once the concentration of the extracted water reaches 2% of the saline water concentration, the well is turned off and the system is allowed to recover. There is no analytical solution for this problem, and thus the accuracy of the axisymmetric simulation approach is assessed by comparing results with other codes. The SEAWAT computer program was used to simulate the problem.

The confined aquifer for this problem is 120 m thick. The upper 98 m is fresh water and the lower 20 m is saline water. A 2-m-thick transition zone separates the fresh water and saline ground water. A partially penetrating well is open to only the top 20 m of the aquifer and pumps at a rate of 2400 m^3/d. The permeability is homogeneous and anisotropic. Permeability in the horizontal direction is 2.56×10^{-11} m^2. Permeability in the vertical direction is 1.0×10^{-11} m^2. The case simulated here is for saline water with a density of 1025 kg m^{-3} (approximately equal to that of sea water), and the longitudinal and transverse dispersivities were set at 1 and 0.5 m, respectively (Zhou et al. 2005, case A). Molecular diffusion was neglected. A constant value of 1×10^{-3} kg/m/s was used for dynamic viscosity.

The finite-difference grid had a similar level of resolution as the finite-element mesh used by Zhou et al.

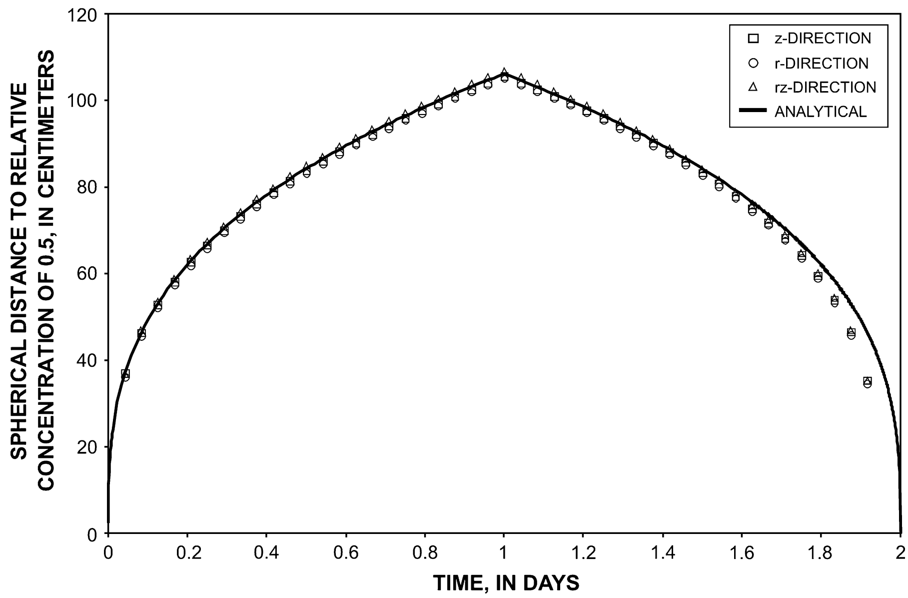

Figure 7. Sphere radius as a function of time for the analytical solution of an expanding and contracting sphere and for the numerical simulation. Results from the numerical solution are shown for the vertical (*z*), radial (*r*), and *zr* (45° angle) directions.

(2005). The grid contains 113 columns and 60 layers. The columns are variably spaced with 0.5-m horizontal resolution near the well expanding to 25-m horizontal resolution at the distant boundary. Each layer is 2 m thick.

The FEAS computer program predicts that the concentration of the extracted water reaches 2% of the underlying saline water after about 3.95 years, whereas SEAWAT predicts that 5.55 years of extraction are required before the 2% salinity concentration is reached (Figure 9). Thus, SEAWAT suggests that 40% more water can be extracted than predicted by FEAS. The same simulation was performed using SUTRA to help resolve the discrepancy between SEAWAT and FEAS, and the SUTRA results compare almost exactly with those of SEAWAT (Figure 9). The cause of the discrepancy was not resolved. One possible explanation is that SEAWAT and SUTRA do not use the same type of solute boundary condition at the distal boundary as the one implemented in FEAS. In FEAS, a concentration gradient of zero is prescribed normal to the boundary, and therefore salt can enter from this boundary only by advection; the concentration of the inflowing water is calculated during the simulation by the model. In SEAWAT and SUTRA, the relative concentration of the inflowing water is specified according to the initial concentrations. Salinity contours from the SEAWAT and FEAS simulations are shown in Figure 10, and the two codes are in good agreement except at the right boundary. This close agreement in

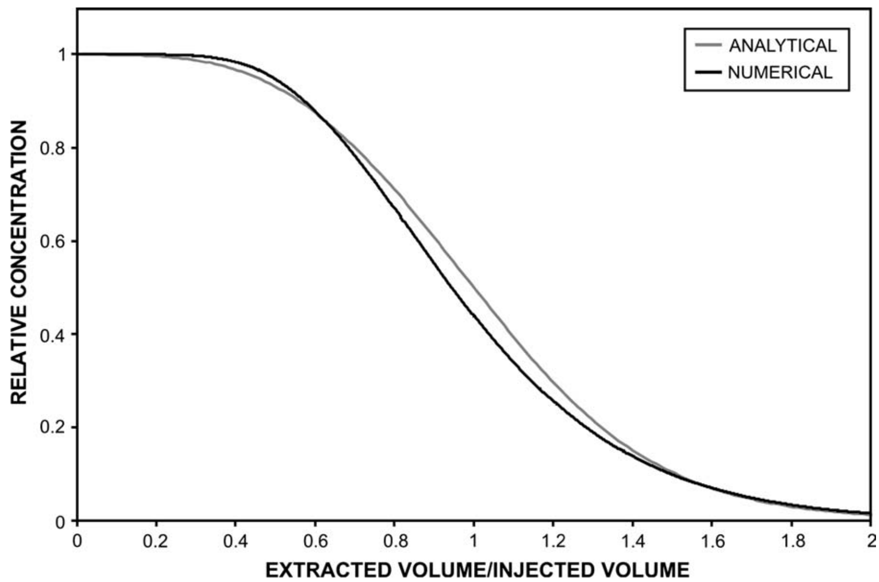

Figure 8. Analytical and numerical breakthrough curves during extraction for the push-pull test example problem.

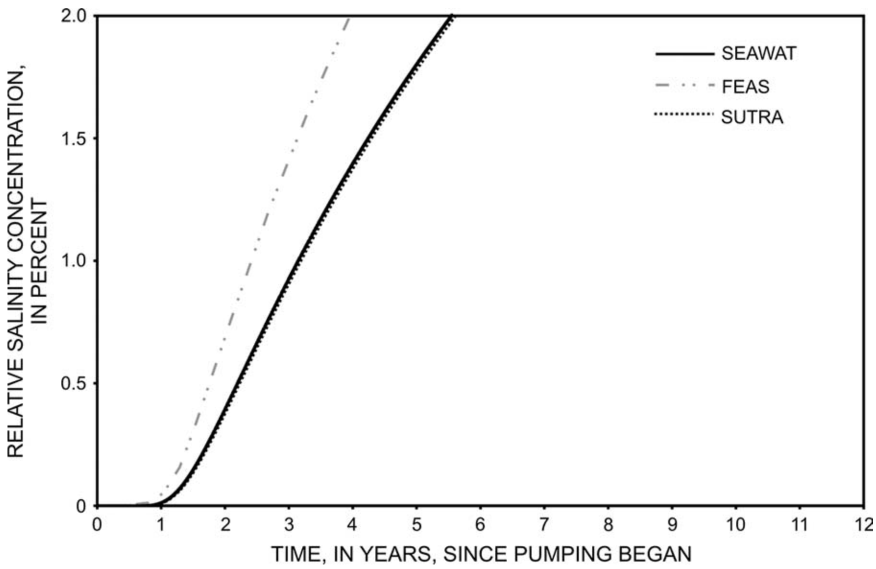

Figure 9. Plot of relative salinity concentration vs. time since pumping began.

salinity contours and the close agreement between SEAWAT and SUTRA for the extracted water concentrations indicate that the axisymmetric approach presented here can be used for variable-density simulations with MODFLOW-based codes, such as SEAWAT.

To assess the computational advantage of the axisymmetric approach over a full three-dimensional representation, a SEAWAT simulation was also performed using a three-dimensional grid. The three-dimensional grid had 60 layers and used the same grid spacing as the two-dimensional grid. Thus, the three-dimensional grid was 225 columns by 225 rows, with the extraction well located at row 113 and column 113. Time stepping, solution tolerances, and other model controls were specified the same as for the axisymmetric model. Results from the three-dimensional model are nearly identical to the axisymmetric results (both SEAWAT and SUTRA) and, therefore, are not shown. On the same computer, the three-dimensional model took more than 2 d to run, whereas the axisymmetric model took about 3 min to run. Thus, for this particular problem, the axisymmetric model was more than 1000 times faster than the equivalent three-dimensional model.

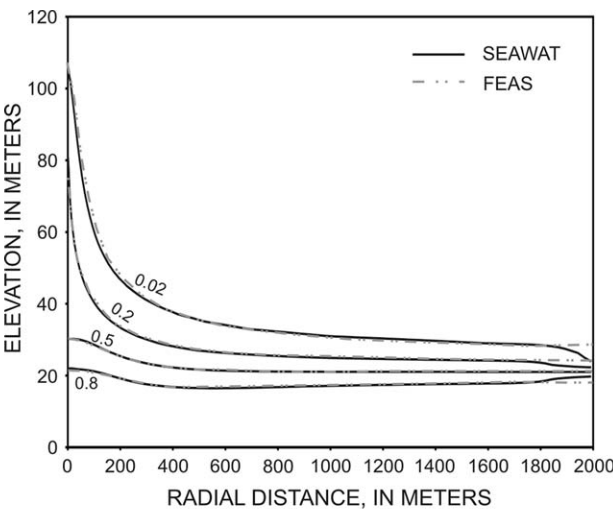

Figure 10. Cross section of relative salinity contours after 3.95 years of pumping.

Discussion and Conclusions

This paper shows that the widely used MODFLOW suite of computer programs can be used to represent axisymmetric ground water flow, transport, and variable-density flow and transport. By adjusting several of the input parameters on a cell-by-cell basis to account for the cylindrical geometry and by selecting the appropriate interblock transmissivity weighting option, MODFLOW is capable of providing accurate simulations of ground water flow. MT3DMS can also be used in its present form to simulate axisymmetric solute transport, provided porosity values are adjusted in a similar manner. The approach is easily extended to variable-density simulations of axisymmetric flow and transport with the MODFLOW/MT3DMS-based SEAWAT computer program. Simulations using the simple approach show good agreement with analytical or finite-element solutions for three test problems: (1) ground water extraction; (2) an aquifer push-pull test; and (3) upconing of saline water into an extraction well. For the upconing problem, the axisymmetric model was more than 1000 times faster than the equivalent three-dimensional model.

Axisymmetric ground water flow and solute transport models run much more quickly than their full three-dimensional counterparts, but their use is not widespread. Part of this lack of use can be attributed to the limiting assumption that flow and transport patterns must be axially symmetric. Another reason axisymmetric flow and transport modeling may not commonly be used is that there is a perception that specialized software packages are required in order to perform the analysis. Evidence of this perception can be found in the literature as axisymmetric conditions are simulated in three dimensions. Recently, three-dimensional flow and transport models have been developed to simulate the effects of aquifer storage and recovery (Brown et al. 2006; Maliva et al. 2006; Vacher et al. 2006) and injection disposal of treated waste water into deep saline aquifers (Maliva et al. 2007). Based on the reported results, these studies would have benefited from the axisymmetric approach presented here. To reduce computer runtimes, Maliva et al. (2006, 2007) used axial symmetry to simulate only one planar quadrant of the problem domain; however, the domain could have been reduced further into only two dimensions. The studies by Brown et al. (2006) and Vacher et al. (2006) describe simulations of aquifer storage and recovery in the presence of a slight regional hydraulic gradient. As noted by Brown et al. (2006), some of the results were questionable due to grid resolution issues. With simple axisymmetric models, appropriate levels of horizontal and vertical resolution may have been quickly identified before moving to time-consuming three-dimensional simulations.

This paper has shown that existing unmodified versions of common computer programs can be used to accurately simulate axisymmetric flow and transport. In addition to the programs used for the simulations described in this paper (MODFLOW, MT3DMS, and SEAWAT), there presumably are other MODFLOW-based programs, such as MODPATH, that could be used to represent ground water processes near an extraction or injection well. Langevin and Zygnerski (2006) showed that the Salt Water Intrusion package for MODFLOW (Bakker 2003; Bakker and Schaars 2003) can be used to simulate interface movement under axially symmetric flow conditions. The clear advantage of the axisymmetric approach presented here is that it is much faster than its full three-dimensional counterpart and it can be used with existing software. Therefore, it has utility for many practical modeling applications such as aquifer hydraulic testing, water resource characterization, aquifer storage and recovery, injection disposal of waste water, and so forth. The approach offers a quick way to determine if more computationally demanding three-dimensional models are necessary and can be used to provide insight into the level of grid resolution required to accurately simulate the hydraulic and water quality responses of an aquifer to an injection or extraction well. The approach could also be used in a preliminary step with parameter estimation programs before developing more complex three-dimensional models.

Acknowledgments

Adam Taylor is thanked for pointing out that the MODFLOW "trick" for representing axisymmetric flow can also be used for MT3DMS and SEAWAT transport simulations. Quanlin Zhou and Mazda Kompani-Zare graciously answered questions regarding the upconing problem and the LSM, respectively. The manuscript was substantially improved by the thoughtful reviews of Alyssa Dausman, Keith Halford, Claire Tiedeman, and Dave Romero. Funding for this work was provided by the USGS Office of Ground Water through the Ground-Water Resources Program.

References

Anderson, M.P., and W.W. Woessner. 1992. *Applied Groundwater Modeling, Simulation of Flow and Advective Transport*. San Diego, California: Academic Press.

Appel, C.A. 1976. A note on computing finite difference interblock transmissivities. *Water Resources Research* 12, no. 3: 561–563.

Bakker, M. 2003. A Dupuit formulation for modeling seawater intrusion in regional aquifer systems. *Water Resources Research* 39, no. 5: 1131.

Bakker, M. and F. Schaars. 2003. The Sea Water Intrusion (SWI) Package Manual, Version 0.2. Athens, Georgia: University of Georgia. http://www.engr.uga.edu/~mbakker/swi.html. Accessed March 9, 2008.

Barlow, P.M., and A.F. Moench. 1999. WTAQ—A computer program for calculating drawdowns and estimating hydraulic properties for confined and water-table aquifers. USGS Water-Resources Investigations Report 99-4225. Northborough, Massachusetts: USGS.

Barrash, W., and M.E. Dougherty. 1997. Modeling axially symmetric and nonsymmetric flow to a well with MODFLOW, and application to Goddard2 well test, Boise, Idaho. *Ground Water* 35, no. 4: 602–611.

Bennett, G.D., T.E. Reilly, and M.C. Hill. 1990. Technical training note in ground-water hydrology: Radial flow to a well. USGS Water-Resources Investigations Report 89-4134. Reston, Virginia: USGS.

Bensabat, J., Q. Zhou, and J. Bear. 2000. An adaptive pathline-based particle tracking algorithm for the Eulerian-Langrangian method. *Advances in Water Resources* 23, no. 4: 383–397.

Brown, D.J., S. England, G.T. Stevens, H.P. Cheng, and E. Richardson. 2006. ASR regional study—Benchscale modeling. U.S. Army Corps of Engineers Technical Report. http://www.evergladesplan.org/pm/projects/project_docs/pdp_asr_combined/082206_asr_benchscale_study.pdf (accessed May 21, 2007).

Cooley, R.L. 1971. A finite difference method for unsteady flow in a variably saturated porous media: Application to a single pumping well. *Water Resources Research* 7, no. 6: 1607–1625.

Diersch, H.J.G. 2002. FEFLOW *Finite Element Subsurface Flow and Transport Simulation System—User's Manual/Reference Manual/White Papers. Release 5.0*. Berlin, Germany: WASY Ltd.

Gelhar, L.W., and M.A. Collins. 1971. General analysis of longitudinal dispersion in nonuniform flow. *Water Resources Research* 7, no. 6: 1511–1521.

Goode, D.J., and C.A. Appel. 1992. Finite-difference interblock transmissivity for unconfined aquifers and for aquifers having smoothly varying transmissivity. USGS Water-Resources Investigations Report 92-4124. Reston, Virginia: USGS.

Guo, W., and C.D. Langevin. 2002. User's guide to SEAWAT: A computer program for the simulation of three-dimensional variable-density ground-water flow. USGS Techniques of Water Resources Investigations Book 6, Chapter A7. Reston, Virginia: USGS.

Halford, K.J., and D. Yobbi. 2006. Estimating hydraulic properties using a moving-model approach and multiple aquifer tests. *Ground Water* 44, no. 2: 284–291.

Halford, K.J., W.D. Weight, and R.P. Schreiber. 2006. Interpretation of transmissivity estimates from single-well pumping aquifer tests. *Ground Water* 44, no. 3: 467–471.

Harbaugh, A.W. 2005. MODFLOW-2005, the U.S. Geological Survey modular ground-water model—The ground-water flow process. USGS Techniques and Methods 6-A16. Reston, Virginia: USGS.

Harbaugh, A.W., and M.G. McDonald. 1996. User's documentation for MODFLOW-96: An update to the US Geological Survey modular finite-difference groundwater flow model. U.S. Geological Survey Open-File Report 96-485. Reston, Virginia: USGS.

Harbaugh, A.W., E.R. Banta, M.C. Hill, and M.G. McDonald. 2000. MODFLOW-2000, the U.S. Geological Survey modular ground-water model: User guide to modularization concepts and the ground-water flow process. USGS Open-File Report 00-92. Reston, Virginia: USGS.

Land, L.F. 1977. Utilizing a digital model to determine the hydraulic properties of a layered aquifer. *Ground Water* 15, no. 2: 15–159.

Langevin, C.D., and W. Guo. 2006. MODFLOW/MT3DMS-based simulation of variable density ground water flow and transport. *Ground Water* 44, no. 3: 339–351.

Langevin, C.D., and M. Zygnerski. 2006. Axisymmetric simulation of aquifer storage and recovery with SEAWAT and the Sea Water Intrusion (SWI) Package for MODFLOW. In *Proceedings of MODFLOW and More 2006, Managing Ground-Water System, Golden, Colorado*, May 22–24, 2006, ed. E. Poeter, M. Hill, and C. Zheng, 465–469. Golden, Colorado: International Ground Water Modeling Center, Colorado School of Mines.

Langevin, C.D., W.B. Shoemaker, and W. Guo. 2003. MODFLOW-2000, the U.S. Geological Survey modular groundwater model—Documentation of the SEAWAT-2000 version with the variable-density flow process (VDF) and the integrated MT3DMS transport process (IMT). USGS Open-File Report 03-426. Reston, Virginia: USGS.

Lebbe, L. 1999. *Hydraulic Parameter Identification: Generalized Interpretation Method for Single and Multiple Pumping Tests*. Berlin, Germany: Springer.

Lebbe, L., and N. van Meir. 2000. Hydraulic conductivity of low permeability sediments inferred from triple pumping test and observed vertical gradients. *Ground Water* 38, no. 1: 76–88.

Lebbe, L., and W. De Breuck. 1997. Analysis of a pumping test in an anisotropic aquifer by use of an inverse numerical model. *Hydrogeology Journal* 5, no. 3: 44–59.

Lebbe, L., and W. De Breuck. 1995. Validation of an inverse model for the interpretation of pumping tests and a study of factors influencing accuracy of results. *Journal of Hydrology* 172, no. 1–8: 61–84.

Lebbe, L., M. Mahauden, and W. de Breuck. 1992. Execution of a triple pumping test and interpretation by an inverse numerical model. *Applied Hydrogeology* 1, no. 4: 20–34.

Maliva, R.G., W. Guo, and T.M. Missimer. 2007. Vertical migration of municipal wastewater in deep injection well systems, South Florida, USA. *Hydrogeology Journal* 15, no. 7: 1387–1396.

Maliva, R.G., W. Guo, and T.M. Missimer. 2006. Aquifer storage and recovery: Recent hydrogeological advances and system performance. *Water Environment Research* 78, no. 13: 2428–2435.

McDonald, M.G., and A.W. Harbaugh. 1988. A modular three-dimensional finite-difference ground-water flow model. U.S. Geological Survey Techniques of Water Resources Investigations, Book 6, Chapter A1. Reston, Virginia: USGS.

Reilly, T.E. 1984. A Galerkin finite-element flow model to predict the transient response of a radially symmetric aquifer. USGS Water-Supply Paper 2198. Reston, Virginia: USGS.

Reilly, T.E., and A.W. Harbaugh. 1993. Computer note: Simulation of cylindrical flow to a well using the U.S. Geological Survey modular finite-difference ground-water flow model. *Ground Water* 31, no. 3: 489–494.

Romero, D.M., and S.E. Silver. 2006. Grid cell distortion and MODFLOW's integrated finite-difference numerical solution. *Ground Water* 44, no. 6: 797–802.

Rushton, K.R., and S.C. Redshaw. 1979. *Seepage and Groundwater Flow: Numerical Analysis by Digital Methods*. New York: Wiley.

Samani, N., M. Kompani-Zare, and D.A. Barry. 2004. MODFLOW equipped with a new method for the accurate simulation of axisymmetric flow. *Advances in Water Resources* 27, no. 1: 31–45.

Schroth, M.H., and J.D. Istok. 2006. Models to determine first-order rate coefficients from single-well push-pull tests. *Ground Water* 44, no. 2: 275–283.

Schroth, M.H., and J.D. Istok. 2005. Approximate solution for solute transport during spherical-flow push-pull tests. *Ground Water* 43, no. 2: 280–284.

Vacher, H.L., W.C. Hutchings, and D.A. Budd. 2006. Metaphors and models: The ASR bubble in the Floridan aquifer. *Ground Water* 44, no. 2: 149–154.

van Meir, N. 2001. Density-dependent groundwater flow: Design of a parameter identification test and 3D-simulation of sea-level rise. Ph.D. thesis, Department of Geology and Soil Science. Ghent University, Ghent, Belgium.

van Meir, N., and L. Lebbe. 2005. Parameter identification for axi-symmetric density-dependent groundwater flow based on drawdown and concentration data. *Journal of Hydrology* 309, no. 1–4: 167–177.

Voss, C.I. 1984. A finite-element simulation model for saturated-unsaturated, fluid-density-dependent ground-water flow with energy transport or chemically-reactive single species solute transport. USGS Water-Resources Investigations Report 84-4369. Reston, Virginia: USGS.

Voss, C.I., and A.M. Provost. 2002. SUTRA, a model for saturated-unsaturated variable-density ground-water flow with solute or energy transport. USGS Water-Resources Investigations Report 02-4231. Reston, Virginia: USGS.

White, M.D., and M. Oostrom. 2000. *STOMP. Subsurface Transport Over Multiple Phases, version 2.0, Theory Guide*. PNNL-12030. Richland, Washington, D.C.: Pacific Northwest National Laboratory.

Zheng, C., and G.D. Bennett. 2002. *Applied Contaminant Transport Modeling*, 2nd ed. New York: John Wiley and Sons Inc.

Zheng, C., and P.P. Wang. 1999. MT3DMS, a modular three-dimensional multispecies transport model for simulation of advection, dispersion and chemical reactions of contaminants in groundwater systems. Vicksburg, Mississippi: Waterways Experiment Station, U.S. Army Corps of Engineers.

Zhou, Q. 1999. Modeling seawater intrusion in coastal aquifers. Ph.D. thesis, Civil and Environmental Engineering Department, Technion-Israel Institute of Technology.

Zhou, Q., J. Bear, and J. Bensabat. 2005. Saltwater upconing and decay beneath a well pumping above an interface zone. *Transport in Porous Media* 61, no. 3: 337–363.